中國機械工程學刊第四十四卷第三期第 261~272 頁(民國一百一十二年)
Journal of the Chinese Society of Mechanical Engineers, Vol.44, No.3, pp261~272 (2023)

Research on the Self-Anti-Interference Control Characteristics of Liquid Hydrostatic Guide Test Bench

Na Lu*, Youmin Wang**, Xu Fang*and Bo Zhu*

Keywords: hydrostatic guide, self-anti-interference control, electro-hydraulic servo control system, oil film thickness

ABSTRACT

The oil film thickness during the work of the machine tool is affected by the load. It is necessary to ensure the accuracy of the guide rail that the thickness of the oil film is maintained in a stable state. The main objective of the present article is to detect the size of the oil film thickness during the working process of the machine tool in real time and simulate the changing cutting force. The mechanical structure of the test bench was designed. The electro-hydraulic servo system schematic was designed and the hydrostatic guide pressure control scheme was determined, the test bench electro-hydraulic servo control system modeling was completed. MATLAB was used to build the simulation model and carry out the corresponding simulation analysis. The self-anti-interference controller completed by the PID control of the fast overshoot pavement self-anti-interference control. To verify the method of this paper, the liquid hydrostatic guide test bench was set up and the corresponding testing experiments were conducted. The simulation and experiments showed that: under the self-anti-interference control environment, the performance of the test bench electro-hydraulic servo control system became better and the oil film thickness tends to be stable.

INTRODUCTION

Liquid hydrostatic guide rail, which is leading the development of modern manufacturing, is an important means to achieve high speed, high precision and high stability in the machinery industry. Hydrostatic guide contains two parameters closely related to the gap oil film thickness, respectively, the oil film stiffness and bearing capacity, the oil film thickness instability will have a negative effect on the oil film stiffness and bearing capacity. Therefore, the important consideration to improve the accuracy of the guide rail is whether the oil film thickness can be maintained in the ideal condition, and the direct method to determine whether the oil film thickness is in the ideal condition is to measure the oil film thickness (Xiao et al. 2021). Li (2020) in order to investigate the influence of different structural design parameters and environmental factors on the performance of the hydrostatic guide, numerical simulation of the internal flow field of its oil cavity was carried out to provide direction and guidance for the design and optimization of the guide system. Cui et al. (2016) analyzed the static and thermal properties of the hydrostatic guide of the machine tool in order to improve the machining accuracy of the precision surface grinding machine. Although the scholars in the above-mentioned literature conducted various academic studies on the influencing factors of the hydrostatic guide of the machine tool, they did not apply them to practice and only stayed at the theoretical level. Rehman et al. (2017) proposed a servo valve and feedback control algorithm to achieve uniform oil film thickness, and did not conduct simulation analysis of the servo valve and feedback control algorithm. In this paper, the simulation of the test bench control system is completed by using the self-anti-interference control algorithm. Han et al. (2019) proposed a feed forward fuzzy adaptive PID anti-interference hierarchical control method for the factors affecting the control accuracy and response speed of constant speed output of variable speed motor under input disorder, but did not introduce this method into the design of liquid hydrostatic guide. Cui et al. (2021) applied fuzzy methods to PID control and added anti-interference techniques in order to solve the problems of low stability, weak anti-interference ability and unsatisfactory response that may be encountered in traditional PID controllers. In this paper, a self-anti-interference control algorithm is introduced using the fast overshoot of PID control to complete the design of the self-

Paper Received June, 2022. Revised , 2022, Accepted October, 2022, Author for Correspondence:. Xu Fang

* *Graduate Student, School of Mechanical Engineering, Anhui Polytechnic University, Wuhu, Anhui 241000, China.*

** *Professor, School of Mechanical Engineering, Anhui Polytechnic University, Wuhu, Anhui 241000, China.*

anti-interference controller. Gong et al. (2020) introduces the DOB anti-interference control theory and improves the anti-interference control algorithm. In this paper, the self-anti-interference control algorithm is introduced using the fast overshoot of PID control and the design of the self-anti-interference controller is completed. Dong et al. (2020) firstly designed a new extended state observer as a predictor to achieve predicted states with total uncertainty representing the unknown nonlinear dynamics and the effect of external perturbations, based on which a predictive self-anti-interference control law was proposed, but the obtained results only provided a solution and guidance, and were not applied to practical cases.

This paper completed the design of the three-dimensional model of the liquid hydrostatic guide test bench and designed the hydrostatic control system of the test bench according to the testing requirements, using AMESim to successfully establish the hydrostatic system simulation model and complete the corresponding analysis. The hydrostatic servo system schematic is established, the transfer function of the electro-hydraulic servo control system is derived and the pressure control scheme of the hydrostatic guide is determined, the simulation model is established using Simulink and the step response performance of the control system is analyzed, and it is concluded that when the system is controlled by PID, it reaches stability at 1.6s but has a certain amount of overshoot. Self-anti-interference controller was designed and tested using a self-interference control algorithm, and the system was found to be stable at 1.2s and the input and output signals matched. Build a test bench for liquid hydrostatic rail and conduct liquid hydrostatic rail oil film thickness testing experiment, simulation and experiments showed that: The deviation of the output force from the input force is within 2N, and the force following is good; the oil film thickness does not differ much when the same loading force is applied at different loading points; the detection accuracy is good. After adding the self-anti-interference control method, the change of oil film thickness of the rail tends to be stable when it is loaded, and the performance of the electro-hydraulic servo system of the test bench is better, and the oil film thickness is controlled stably.

LIQUID HYDROSTATIC GUIDE MODELING AND TEST BENCH HYDRAULIC CONTROL SYSTEM DESIGN

3D modeling of the liquid hydrostatic guide

The mechanical part of the oil film thickness inspection test bench is designed with two moving modules, horizontal and vertical, to simulate the variation of cutting force of machine tools.

As can be seen from the Figure 1, the mechanical structure of the test bench includes two parts: horizontal moving module and vertical moving module. The horizontal moving module is powered by electric motor to drive the dynamic guide rail to make horizontal linear motion along the static guide rail direction, and the vertical moving module uses electro-hydraulic servo control system to drive the piston rod to apply different loads to the dynamic guide rail, so as to complete the simulation of machine cutting force. The first motor is powered, and the first coupling is used to drive the ball screw nut assembly to move, and then push the dynamic guide operation. At this time, the motor bracket plays a supporting role for the first motor and the first coupling, and when the first coupling connects the first motor shaft and the first ball screw shaft end, the first motor transmits the power to the first ball screw. The first ball screw clamping nut locks the through wire outer joint, therefore self-locking through the friction between the bolt nut and locking the bearing to achieve the purpose of eliminating the clearance. The handle provides the driving force through rotation, and this driving force drives the second ball screw to rotate forward and backward. The handle bracket is assembled between the handle and the second ball screw, which plays the role of supporting the two. The mechanism can convert the horizontal movement into vertical movement through the connecting rod. When it moves vertically, the second slider on the column through the action of the connecting rod sliding up and down, and then the second slider on the fixed hydraulic cylinder together with the vertical movement. At the same time, take to adjust the valve spool opening and direction to make the piston rod work, and then complete the dynamic guide variable force loading.

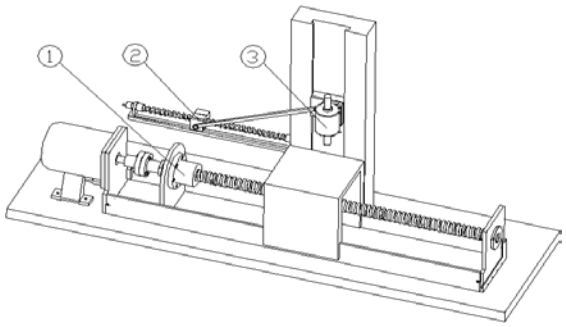

Fig. 1. 3D model of the mechanical structure of the test bench. 1- Horizontal movement module, 2 - Vertical movement module, 3 - Mechanical structure

Design of hydraulic control system for test bench

The hydraulic control system contains electro-hydraulic force servo control system and oil film thickness detection system, of which, the electro-hydraulic force servo control system consists of electro-hydraulic force servo control circuit and oil supply system, and the principle of hydraulic control system is shown in the Fig.2.

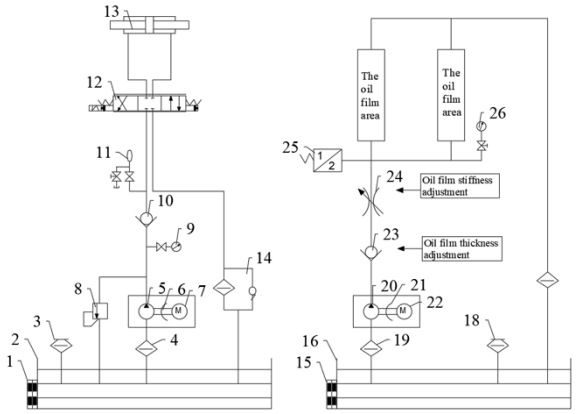

Fig.2. Hydraulic control system schematic. 1-first level gauge,2-first oil tank,3-first air filter, 4-relief valve,5-first suction filter,6-first constant pump,7-first coupling,8-first motor,9-first hydraulic gauge assembly,10-first check valve,11-accumulator,12-electrohydraulic servo valve,13-hydraulic cylinder,14-return filter, 15-second check valve,16-throttle valve,17-pressure sensor,18-second hydraulic gauge assembly,19-strainer.

The selection of hydraulic system components is mainly divided into standard components and special components, on the basis of meeting the system requirements, the hydraulic system components is try to use standard parts to shorten the manufacturing cycle (Lai et al., 2021), the rated pressure of the hydraulic system in this paper is 6, the nominal pressure is 10, the piston rod left and right stroke are 100.

Hydraulic pump specifications: Pump specifications selected, the first requirement is to know the maximum operating pressure and flow rate of the system cylinder. Since there is loss in the oil circuit during operation, the maximum operating pressure of the pump is the formula (1).

(1)

Where △p is the total pressure loss from the pump oil supply to the oil entering the cylinder. The pressure loss of common pipeline is 0.2-0.5, and the pressure loss of complex pipeline is 0.5-1.5, here it is 0.5. Specify the style of the pump, the first thing to know that the maximum operating pressure obtained from the formula (4-5) is only the operating pressure when the system is static, rather than dynamic operating pressure. In order to enable the pump to have a considerable reserve pressure, dynamic operating pressure than static to be higher, usually the pump pressure rating for its static operating pressure of 1.25-1.6 times. The rated pressure of the hydraulic pump is the formula (2).

(2)

The flow rate of the hydraulic pump is the formula (3).

(3)

Where is the system leakage coefficient, which is usually taken 1.1-1.3; is the actuator maximum flow rate. When the operation has a relief valve regulation, need to add at least the relief flow, so there is the formula (4).

(4)

When the leakage factor of the system , the maximum flow rate of the pump is the formula (5).

(5)

Known and, the CBGF1018 gear pump is selected.

Electro-hydraulic servo valve specifications: The oil supply flow rate at maximum power is the formula (6).

Table 1. Hydraulic component selection table

Hydraulic components	Component Parameters	Part specification model
Hydraulic cylinder	D=63*mm* d=35*mm*	
Hydraulic Pumps		*CBGF1018 gear pump*
Electric motors	Rated power 5.5 *kW*, full load speed is1440r/*min*	*Y series three-phase asynchronous motor Y2-132S-4*
Electro-hydraulic servo valve	Rated flow rate 20*L/min*	*4WSE2EM6-2X*
One-way valve	Rated flow rate 30*L/min*	*RVP10-30B*
Servo Amplifier		*NB2000*
Relief valve	Rated flow rate 30*L/min*	*DBDS6G10/200*
Pressure sensors	Measuring range 0~1000*kg*, voltage 0~10*V*	
Pipeline (Seamless steel pipe)	Inner diameter 16*mm*, wall thickness 2*mm*	
Fuel tank	V=68.28*L*	

(6)

If leakage is factored in, there is the formula (7).

(7)

The total pressure drop across the valve port is the formula (8).

(8)

Bywithcan be selected servo valve specifications for Rexroth servo valve, model 4WSE2EM6-2X, its pressure drop is when the rated flow is 20, the maximum operating pressure is 20 , the rated current is.The inherent frequency of the servo valve, damping ratio. It has a gain of the formula (9).

(9)

Table 1 lists the various component options.

Hydraulic control system simulation

The hydraulic control system is modeled and simulated using AMESIM (Tomoaki et al., 2018), and the simulation model is shown in Fig.3.

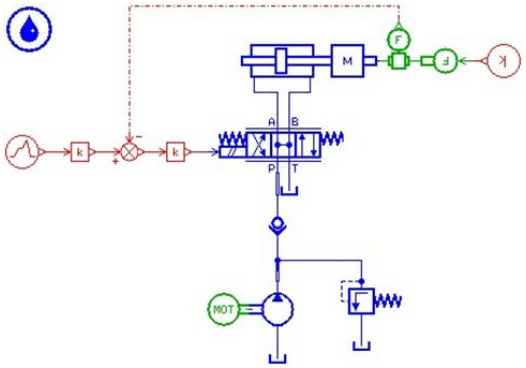

Fig.3. Hydraulic control system simulation model diagram

By adjusting the parameters of each component, the dynamic performance of the system is continuously optimized, thus improving the efficiency of the equipment. When the hydraulic control system simulation in the parameter mode, refer to the selection of hydraulic control system components to complete the setting of each component parameters. Enter the simulation through Simulation mode in AMESIM (Deng et al., 2021: Li et al., 2022), set the run parameters by Set the run parameters, open the Run parameters frame, set the Final time for cylinder inlet pressure and flow rate to 0.5 seconds, set the Final time for oil film thickness compression to 0.03 seconds, and Communication interval is set to 0.01 seconds, the rest of the default value is used, the simulation is carried out by Start a simulation, and the simulation results are obtained.

Through the Variable List of piston rod and dynamic guide can see the simulation results, the flow rate of the cylinder inlet when the guide is loaded as shown in the Fig.4, the flow rate of the cylinder oil instantly increased to the maximum, with the loading by the oil film reaction force increasing flow rate gradually becomes smaller, until the thickness of the compression of the maximum when the loading is completed, the flow rate drops to zero. When the guide rail is loaded, the cylinder inlet pressure is shown in the Fig.5, when the oil film is just loaded, the total force of the oil film is instantly very small, the cylinder inlet pressure is also very small, with downward loading gradually, the oil film resistance soon increases, the cylinder inlet pressure also soon increases, but by the role of the relief valve, the pressure will not be infinitely large, will slightly increase, and then basically remain unchanged.

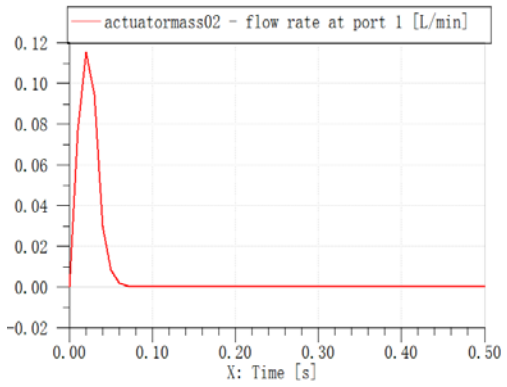

Fig.4. Flow rate change at the inlet of the cylinder

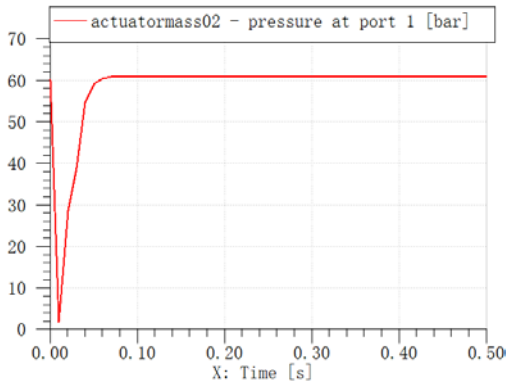

Fig.5. Pressure change at the inlet of the cylinder

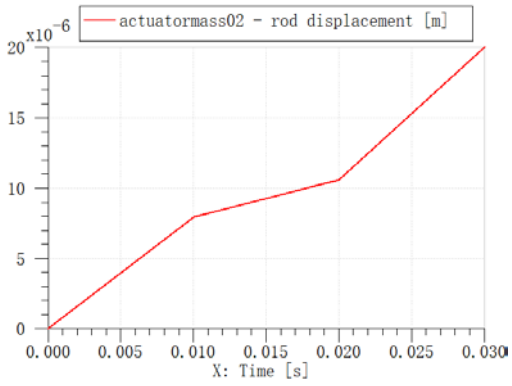

Fig.6. Oil film thickness compression amount change graph

The dynamic guide is squeezed downward under load and the oil film thickness is compressed as shown in the Fig.6, the oil film thickness is subjected to load and its compression reaches a set 20 micron.

ELECTRO-HYDRAULIC SERVO CONTROL SYSTEM OF TEST BENCH

Modeling of electro-hydraulic servo control system for test bench

The oil film thickness control system is the guarantee of the oil film thickness in a stable condition. The system regulates the variable load from the vertical moving module, making the oil thickness between the moving and static guide relatively stable. The schematic diagram of the electro-hydraulic servo control

system of the test bench is shown in Fig.7. The block diagram of the machine's hydrostatic guide control system is shown in the Fig.8.

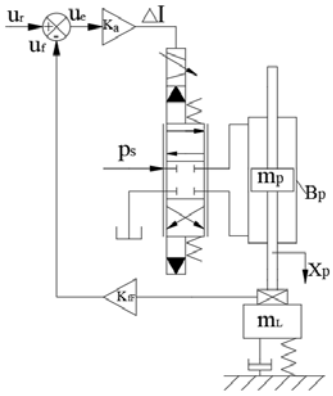

Fig.7. Schematic diagram of electro-hydraulic servo control system

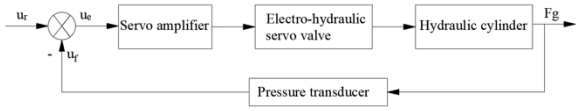

Fig.8. Block diagram of 8 machine tool hydrostatic guide control system

When the system input voltage signal, the actuator hydraulic cylinder piston rod will produce force and loaded on the dynamic guide, at this time the pressure sensor to accept the force and into a feedback voltage signal, the difference between this feedback voltage and input voltage through the servo amplifier conversion and amplification into the electro-hydraulic servo valve, so that it is powered to drive the electro-hydraulic force servo control circuit work, take the adjustment of the valve spool opening and direction to make the piston rod move, and then change the load force applied to the dynamic guide until the output force is equal to the value corresponding to the input voltage signal, thus detecting the change of oil film thickness of the test bench is similar to the change of oil film thickness of the machine tool cutting process.

Modeling of electro-hydraulic servo control system for test bench

For the purpose of this paper, it is necessary to establish the hydraulic control valve flow equation, the cylinder flow continuity equation and the force balance equation between the cylinder and the load. In this paper, we choose a zero-opening four-sided slide valve, which has four symmetrically distributed throttle ports, and the supply pressure of this valve is kept constant with no return pressure. The flow equation of the control valve is the formula (10).

(10)

Where is the load flow rate []; is the flow gain factor []; is the spool displacement []; is the flow-pressure gain coefficient []; is the load pressure [].

Usually, the leakage involved in the cylinder belongs to the laminar flow, and its pipeline with the servo valve is rough and short, and the pressure loss in the process is often not counted. The cylinder flow continuity equation is the formula (11).

(11)

Where is the effective working area of the cylinder []; is the rod displacement []; is the total leakage coefficient of the cylinder [], and ; is the In-cylinder leakage coefficient; is the external leakage coefficient of the cylinder; is the total compressed volume []; is the effective bulk modulus of elasticity [].

The load affecting the performance of the system cylinder usually contains elastic force, damping force and inertia force. The equation of force balance between cylinder and load is the formula (12).

(12)

Where is the load frequency [];
is the load damping coefficient [];
is the load spring stiffness [].

Equation (10), (11) and (12) explain the dynamic performance of the valve-controlled cylinder, and the formula (13) can be obtained by Laplace transform.

(13)

Where
is the load frequency [], ;
is the stiffness damping ratio, ;
is the natural frequency of coupling stiffness and load mass [], ;
is the damping ratio, ;
is the total pressure gain [];
is the cylinder output force [];
is the spool displacement [];
is the cylinder effective working area [].

From equation (13), the simplified block diagram of the control system is shown in Fig.9.

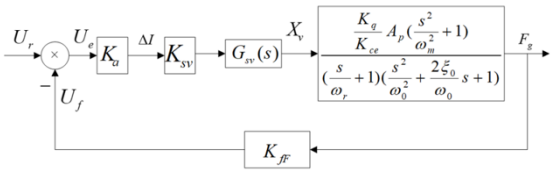

Fig.9. Simplified block diagram of the control system

Because , from the selected components, the parameters of equation (13) are assigned and simplified to obtain the transfer function as:

The input-output differential equation of the system, the formula (14) can be obtained from the transfer function.

(14)

By simplifying, we get the formula (15).

(15)

Since, so the state space representation corresponding to equation (7) is:

=

Simulation analysis of electro-hydraulic servo control system

The Simulation model control system is performed by Simulink (Xue, 2022). In the Simulink environment, the simulation is taken for the system transfer function and the resulting system step response curve is shown in Fig.10.

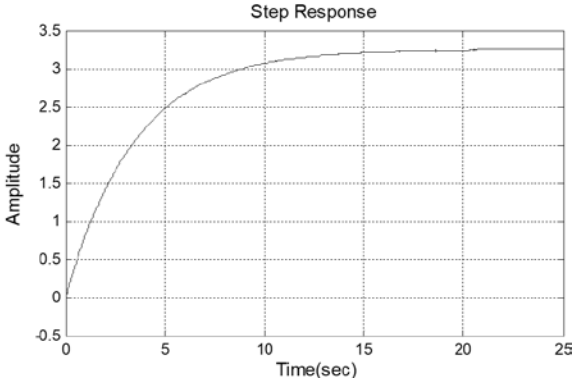

Fig.10. System step response curve

As can be seen from the Figure 10, the control performance of the system is very unsatisfactory, when the input unit step signal, the system can be stabilized in about 20.5s, which is a long time, and its input and output signals do not match, which needs to be optimized. In the Simulink environment, the servo system PID control simulation model is created as shown in Fig.11. The PID control step response curve of the system using Simulink simulation is shown in Fig.12.

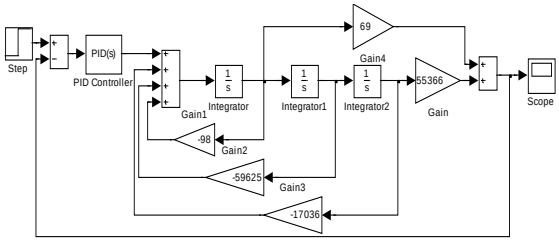

Fig.11. System PID control simulation model diagram

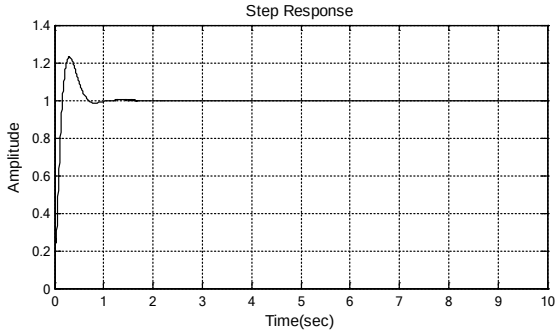

Fig.12. System PID control step response curve

The Fig.12 shows that the performance of the system is improved somewhat with PID control (Miroslav K, 2017). The system stabilizes at 1.6s when a unit step signal is input, and its input and output signals match. However, the fast response of the system is accompanied by a certain amount of overshoot, which needs to be improved to optimize the control.

TEST BENCH ELECTRO-HYDRAULIC SERVO CONTROL SYSTEM INTELLIGENT SELF-ANTI-INTERFERENCE CONTROL

For the complexity of the electro-hydraulic servo control system, a self-interference control algorithm is proposed to optimize the control system performance, and the specific structure of the self-interference controller is analyzed and designed. In order to further improve the control effect of the test bench control system and enhance the overall performance of the system, this paper adopts a comprehensive optimization of the classical PID control based on the self-interference control algorithm. Classical PID control has been widely used because of its simple structure and convenient parameter calibration (Miroslav, 2017). In order to improve the performance of the test bench control system, a PID controller is added to the system, and the difference between the initial value v(t) and the output value y(t), e(t), is applied to the controlled object through proportional, integral and differential links to obtain the optimized results, and the schematic diagram of the PID controller is shown in Fig.13.

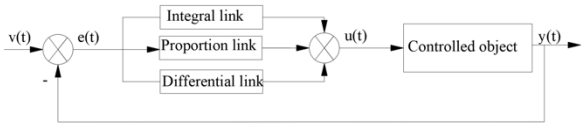

Fig.13. PID controller schematic

As can be seen from the Figure 13, the PID control includes the PID controller and the controlled object, and the object referred to here is the test bench servo system. The relationship between the initial input v(t) and the actual output y(t) of the controller is the formula (16).

(16)

This results in the transfer relation of the PID controller as shown in the formula (17).

(17)

Where is the proportional gain; is the time constant of integration; is the differential time constant. The proportional coefficient is first determined, so that the integration constant and differential constant are 0, the proportional gain will gradually increase from zero to the response curve oscillation, and then slowly reduce the data until the oscillation

stops, take 30%-70% of the proportional gain as the system proportional coefficient, The value here is 60%. After the proportional coefficient is decided, the larger value is selected as the initial value of the integration constant of the system, and through repeated adjustment, the system stops oscillating, and 150%-180% of the integration constant is taken as the final value of the integration constant of the system, which is taken as 165% at this time. In the case of the system output force, the differential constant is dusually chosen 0. Ultimately, the parameters of the PID controller are chosen as ,,, respectively. The block diagram of the self-anti- interference control analyzed in this paper is shown in Fig.14.

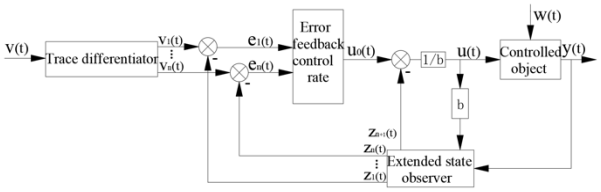

Fig.14.Block diagram of self-interference control

The self-interference controller includes three modules, firstly, the tracking differentiator (TD) gives a suitable transition process to the system input value, which better solves the problem of fast response of the system with overshoot during classical PID control, and realizes fast response to the tracked system input value without overshoot. In addition, it can also regulate the error differential signal, and the differential form of the given signal is obtained from the order of the controller. Secondly, the expansion state observer (ESO) is used to represent the integral feedback of the error and to observe the derivatives of each order of the system output in real time so as to evaluate the system perturbations. Third, the control law (CL) effectively evaluates the system given signal as well as the error signal from the dilated state observer and compensates the system perturbations monitored by the dilated state observer in real time.

Intelligent self-anti-interference controller design

It is known from the system state space expression that the controlled object is of third order, so the tracking differentiator is of third order and the dilated state observer is of fourth order. The structure of the third-order self-anti-interference controller is shown in Fig.15. The zero-pole diagram of the controlled object is derived from the simulation as shown in Fig.16.

As can be seen from the Figure 16, the system model has no zeros and poles in the positive part of the complex plane, so it belongs to the minimum phase system. At this time, it is able to determine the virtual control quantity by the self-anti-interference controller, and then the virtual control quantity as the input to solve the system to get the actual control quantity.

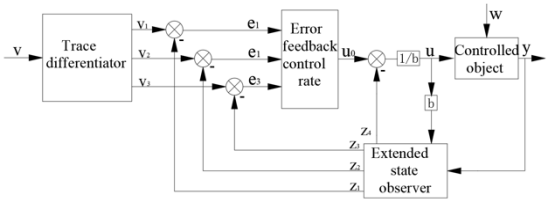

Fig.15.Third-order self-interference controller structure diagram

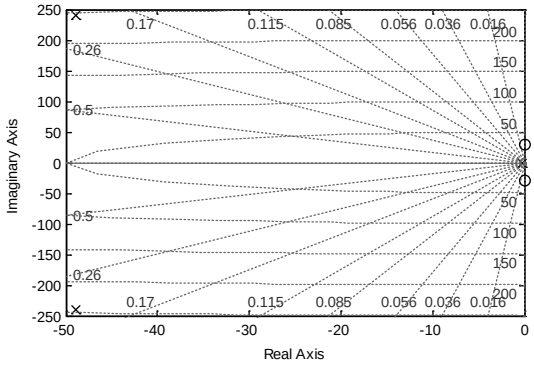

Fig.16. The zero-pole diagram of the accused object

By the control system transfer function is known to satisfy the cubic polynomial , and at this time the parameters ,andknown, the algorithm of the third-order tracking differentiator can be obtained as the formula (18).

(18)

Where is the rapidity factor; is the sampling step. ESO is a fourth-order dilated state observer, and the control system fourth-order dilated state observer algorithm is the formula (19).

(19)

Where are the expansion state observer parameters; is the error term. In the control system, ESO contains four output variables, following the system output , following , following , which form the feedback part of the self-interference controller, following the system integrated disturbance and using feed-forward methods to compensate for the disturbance (Chao et al., 2021).The transfer relation from input to output of the expansion state observer is the formula (20).

(20)

In order to achieve a certain estimation accuracy, it is necessary to choose a larger gain coefficient, i.e., the gain coefficient needs a larger value so as to satisfy the high gain observer mode. The error feedback control law compares the state variables obtained from the transition process, each order of differentiation and the dilated state observer for a given signal of the system, and then the deviation signal is algorithmically derived from the control quantity (Liu et al., 2021). The algorithm is the formula (21).

(21)

The algorithm for the final control volume is the formula (22).

(22)

Simulation of self-anti-interference control of test bench electro-hydraulic servo control system

The test bench electro-hydraulic servo control system combined with Simulink module to establish the control system self-anti-interference control simulation model (Wang et al., 2019), as shown in Fig.17.

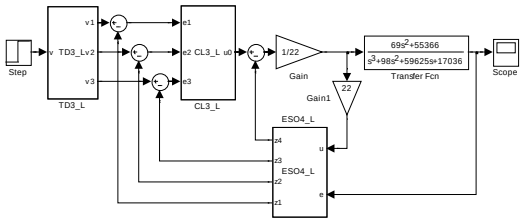

Fig.17. Self-anti-interference control simulation model of control system

The parameter r in the tracking differentiator has the greatest influence on its performance (Jin, 2020). increases, decreases the time to arrange the transition process, increases the overshoot of the system, and the tracking effect becomes better. cannot be too large, otherwise the signal quality of the tracking differentiator will become poor. becomes smaller, increases the time to arrange the transition process, decreases the overshoot of the system, and the tracking quality becomes poor. cannot be too small, otherwise the tracking effect of the system will become poor.

The dilated state observer parameters , ,and affect its dynamic characteristics. Whenincreases, the system does not have much effect; when decreases, the system will have divergent oscillations. When becomes large, the system emits a noise signal, which leads to a decrease in the control performance of the system; when becomes small, the system will increase the number of oscillations and the amplitude increases. When becomes large, it will increase the number of oscillations and the amplitude becomes larger; when becomes small, the system tracking time becomes longer and the oscillation amplitude gradually becomes smaller. When becomes larger, the system oscillation amplitude becomes larger and the tracking speed slows down; when decreases, the tracking speed of the system slows down substantially and even causes phase lag.

The parameters , and of the error feedback control rate have an impact on its performance. Whenbecomes large, the system overshoot increases and makes its control quality decrease; when becomes small, the system response is lower than the given signal and the tracking effect is poor. When becomes large, the response is lower than the given signal, and the tracking effect is poor; when becomes small, the system oscillates and the amplitude decreases slowly. When becomes large, the system response is good; when decreases, the system will slightly overshoot.

Set the parameters of the three modules of the controller separately, with: TD: ESO:; CL: . With Simulink simulation, the control system self-anti-interference control step response curve is shown in Fig.18.

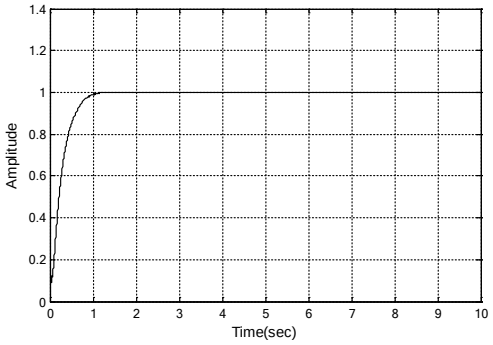

Fig.18.Self-anti-interference control step response curve of control system

As can be seen from the Figure 18, the performance of the servo system self-anti-interference control is significantly improved. The control system is stable at 1.2s when the unit step signal is input, and its input and output signals match. It can be concluded that the performance of the servo system has been greatly improved after self-interference optimization.

TEST BENCH CONSTRUCTION AND EXPERIMENT

Test bench construction

The test bench is hydraulic cylinder driven type, with the overall structure of traditional machine tool, equipped with PLC touch screen and hydraulic control system. The oil film thickness of the test bench is measured by indirect measurement method and converted into the corresponding distance value by PLC calculation. Main machine length*width*height=1200 *800*1500; console length*width*height=800*500* 1000; oil film dynamic guide length is 800, left and right stroke each is 100 (Huaichao et al., 2018).

The general assembly diagram of the test bench is shown in the Fig.19, the test bench dynamic guide contains 6 oil supply cavity, by supplying oil to 6 the oil supply cavity at the same time to jointly support the suspension of the dynamic guide, the test bench loading hydraulic cylinder through the servo valve to simulate the actual working process of the machine tool downward vibration force, through the reversing valve to control the piston movement of the reversing hydraulic cylinder, so as to drive the dynamic guide to do horizontal reciprocating motion, the test bench reversing hydraulic cylinder As shown in the Fig.20 (Wu et al., 2019).

Fig.19. General assembly of the test bench

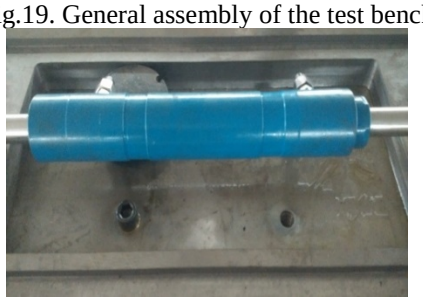

Fig.20. Hydraulic cylinder for reversing the test bench

Test bench testing experiments

Firstly, the oil film stiffness and thickness are adjusted, and then the loading cylinder can be controlled by PLC to complete the loading experiment (Andreas, 2017; Sun et al., 2021). When the oil film stiffness and oil film thickness adjustment is completed, the loading hydraulic cylinder can be controlled by PLC to do the loading experiment. In the experimental process, the PLC controls the computer,

As can be seen from Table 2, the deviation between the output force at point a and the input force is within 2N. From the oil film thicknesses of the five points in Table 2, it can be seen that there is not much difference in the oil film thickness at different loading points with the same loading force. The oil film thickness variation curves before and after the self-anti-interference control are shown in Fig.21.

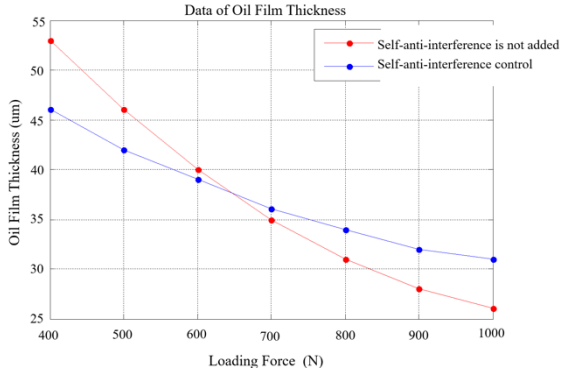

Fig. 21. Oil film thickness change curve

CONCLUSIONS

In this paper, the hydrostatic control system of the test bench is designed, the hydrostatic control system is simulated and analyzed, the hydrostatic guide pressure control scheme is determined, the modeling of the electro-hydrostatic servo system of the test bench is completed and the corresponding simulation analysis is completed. The self-anti-interference controller completed by the PID control of the fast overshoot pavement self-anti-interference control. The simulation of the test bench control system was completed by the self-anti-interference controller. The results show that the performance of the servo system after self-interference optimization has been greatly improved. The design and assembly of each part of the test equipment are completed. The experiments included the force following and gap detection accuracy, the relationship between force and oil film thickness, then the relationship between force and oil film thickness at different action points, and the change of oil film thickness before and after the optimization of self-interference control. The experimental results show that: The deviation of the output force from the input force is within 2N, and the force following is good; the oil film thickness does not differ much when the same loading force is applied at different loading points; the detection accuracy is good. After adding the self-anti-interference control method, the change of oil film thickness of the rail tends to be stable when it is loaded, and the performance of the electro-

accepts the signal input and generates the corresponding algorithm to get the control signal through signal conversion and amplification to adjust the servo valve, the servo valve regulates the upper cylinder to generate the loading force, so that the output force follows the input loading force signal. By inputting different forces at point a, detecting the corresponding output force, using a micrometer to measure the oil film thickness at point a when loaded, and observing the oil film thickness at this time through the display, optimizing by self-anti-interference control, detecting the oil film thickness at point a when loaded, changing the position of point a, and observing the oil film thickness of the display at points b, c, d, and e, respectively, and the detected experimental values are shown in the Table 2. The detected experimental values are shown in the Table 2. By constantly changing the position of the measurement point and repeating the test, the corresponding oil film thickness is measures. As can be seen from the Fig. 21. In the range of 400~1000N, the slope of the oil film thickness change curve is large when the self-anti-interference control is not added, the oil film thickness change is more drastic, after the self-anti-interference control is added, the slope of the oil film thickness change curve is small, the oil film thickness change is more stable. Therefore it can be seen that adding the self-anti-interference controller, the change of the oil film thickness of the rail is much slower when it is under load, making the oil film thickness more stable.

hydraulic servo system of the test bench is better, and the oil film thickness is controlled stably.

Table 2. Test experiment values

a Input force (*N*)	a Output force (*N*)	a Micrometer oil film thickness (*um*)	a Display oil film thickness (*um*)	a Self-interference control oil film thickness (*um*)	b Display oil film thickness (*um*)	c Display oil film thickness (*um*)	d Display oil film thickness (*um*)	e Display oil film thickness (*um*)
400	402	52	53	46	53	54	52	53
500	499	45	46	42	45	47	46	47
600	600	40	40	39	41	39	40	41
700	702	36	35	36	34	36	36	35
800	798	31	31	34	31	33	32	31
900	901	27	28	32	27	28	28	29
1000	999	26	26	31	26	25	24	27

AUTHOR CONTRIBUTIONS

Na Lu had made substantial contributions to design, experimental research, data collection and result analysis; Youmin Wang made critical changes to important academic content; Xu Fang and Bo Zhu made the final review and finalization of the articles to be published.

DATA AVAILABILITY

The data used to support the findings of this study are included within the article.

FUNDING STATEMENT

This article belongs to the project of the "The University Synergy Innovation Program of Anhui Province (GXXT-2019-004)" "Natural Science Research Project of Anhui Universities (KJ2021ZD0144)" "Science and Technology Planning Project of Wuhu City (2021YF58)."

CONFLICTS OF INTEREST

The authors declare that they have no conflicts of interest to report regarding the present study.

REFERENCES

Andreas, I., Ahmed., Theofilos, A., et al., "Papadopoulos, Andreas I, et al. MIMO-OFDM narrowband-PLC in distribution systems: Impact of power transformers on achievable data rates" [J]. *Electric Power Systems Research*, Vol.151, pp.251-265(2017).

Cui, Y. and Guo, C.S., "Study on the Hydrostatic Slide Film Temperature Field and Bearing Capacity of Precision Grinding Machine". *Proceedings of the 5th International Conference on Electrical Engineering and Automatic Control*, Vol.367, No.6,pp. 717-724. (2016).

Cui, Y.Y., Gao, X.Y., Wang, S.Z., et al., "Anti-interference control of servo motor system based on intelligent fuzzy PID" [C] *4th International Symposium on Power Electronics and Control Engineering*, Vol.12080, pp. 552-558(2021).

Chao, S., and Wei, S., "An extended state observer-based control design for electro-hydraulic position servomechanism" [J]. *Control Engineering Practice*, Vol.109, No.104730(2021).

Dong, C.Y., Ran, M.P., Wang, Q., et al., "Active disturbance rejection control for uncertain time-delay nonlinear systems". *Automatica*, Vol.112, No. 108692 (2020).

Deng, B.H., Feng, K.L., and Zha, C.Z., "An AMESIM-based simulation of hydraulic system design for ultra-high pressure tablet presses" [C]. *Journal of Physics: Conference Series*, Vol.1983, No.1, pp.22-24 (2021).

Gong, Y.F., Wang, Y.M., and Yan, Z.C., "Research on Anti-interference Control of Hydrostatic Guide Rail's Oil Film Thickness" [J]. *ManufacturingTechnology*, Vol.20, No.6, pp.849-861 (2020).

Han, X.P., Su, W.B., Zhao, H., et al. "Research on the hydrostatic transmission for deep-sea current energy converter". *Computer Science 2019 IEEE 8th International Conference on Fluid Power and Mechatronics (FPM)*, Vol.207, No.112544 (2019).

Jin, J.Z., Design and Application Research of Improved Active Disturbance Rejection Controller[D]. *Heifei University of Technology*, Vol.2, No.001304(2020).

Liu, F.C., Wang, L.X., Zhao, D.X., et al., "Linear active disturbance rejection control for a class of electro-hydraulic position servo system with light load" [J]. *Control Theory & Applications*, Vol.38, No.4, pp.503-515(2021).

Lai, L.H., Sun, X.D., Zhu, Z., et al., "Design and Analysis of a Novel Mechanic-Electronic-Hydraulic Powertrain System for Agriculture

Tractors" [J]. *IEEE Access*, Vol.9, pp.153811-153823(2021).
Li, M.J., Wang, Z.L., and Zheng, H.B., "Simulation and optimization for pressing system of hydraulic brick press based on AMESim" [C]*Journal of Physics: Conference Series*, Vol.2187, No.012026(2021).
Li, Y.X., "Analyzing the Flow Field in the Oil Chamber of a Hydrostatic Guide Rail Used for Ultra-Precision Machining: Numerical Simulation and Performance Optimization" [J]. *Fluid Dynamics & Materials Processing*, Vol.16, No.6, pp.1129-1145(2020).
Miroslav, K. "On the applicability of PID control to nonlinear second-order systems" [J]. *National Science Review*, Vol. 4, No.5, pp.668(2017).
Rehman, W. U. et al., "Control of an oil film thickness in a hydrostatic journal bearing under different dynamic conditions." *2017 29th Chinese Control and Decision Conference (CCDC), Chongqing, China*, pp. 5072-5076 (2017).
Sun, G.C., Wang, K.P., Wu, H.C., et al., "Influence Study of Oil Film Thrust Bearing on Thermal Characteristics of High-speed Precision Roll Grinding Head" [J]. *Manufacturing Technology*, Vol.18. No.2, pp. 330-336(2018).
Sun, X., and Zhai, X., "Research on PLC System Design of a New Type of Rotary Tilier Control Parameters (Programmable Logic Controller)" [J]. *INMATEH-Agricultural Engineering*, Vol. 64, No.2(2021).
Tomoaki, K., and Yoshinobu, Y., "Directnumerical simulation of liquid metal free-surface turbulent flows imposed on wall-normal magnetic field" [J]. *Fusion Engineering and Design*, Vol.136, pp.925-930(2018).
Wu, H.C., Zhao, L.M., Yan, W.M., et al., "Design and Dynamic Performance Study on Hydrostatic Lubrication System of High-speed Precision Roller Grinding Head" [J]. *Manufacturing Technology*, Vol.19, No.6, pp.959-965(2019).
Wang, D., Yang, Y.Y., Zhang, T., et al., "Investigation of the liquid film thickness in an open-channel falling film micro-reactor by a stereo digital microscopy" [J]. *Journal of the Taiwan Institute of Chemical Engineers*, Vol.98, pp.27-36(2019).
Xue, D., Modeling and Simulation with Simulink®: For Engineering and Information Systems[M]. Walter de Gruyter GmbH & Co KG, 2022.
Xiao, D.L., Zhang, C., Fang, B.W., et al., "Analysis of Liquid Hydrostatic Guide Technology," *Mechatronics Information*, Vol. 20, No.7, pp. 51-52 (2021).

NOMENCLATURE

the total pressure loss
the system leakage coefficient
the actuator maximum flow rate
the load flow rate
the flow gain factor
the spool displacement
the flow-pressure gain coefficient
the load pressure
the effective working area of the cylinder
the rod displacement
the total leakage coefficient of the cylinder
the In-cylinder leakage coefficient
the external leakage coefficient of the cylinder
the total compressed volume
the effective bulk modulus of elasticity
the load frequency
the load damping coefficient
the load spring stiffness
the load frequency
the stiffness damping ratio
the natural frequency of coupling stiffness and load mass
is the damping ratio
the total pressure gain
the cylinder output force
the spool displacement
the cylinder effective working area
the proportional gain
the time constant of integration
the differential time constant
the rapidity factor
the sampling step
the expansion state observer parameters
the error term

液體靜壓導軌試驗臺自抗擾控製特性研究

盧娜 王幼民 方旭 朱波
安徽工程大學機械工程學院

摘要

機床工作過程中油膜厚度受載荷影響，維持油膜厚度居於穩定狀況是保證導軌精度的必要環節。為了能夠實時檢測機床工作過程中油膜厚度的大小，能夠模擬出變化的切削力，本文設計了試驗臺機械結構，建立了電液力伺服系統原理圖並確定靜壓導軌壓力控製方案，完成了試驗臺電液力伺服控製系統建模，使用 Matlab 建立模擬模型並進行相應的模擬分析，由 PID 控製的快速超調鋪墊自抗擾控製，設計完成了自抗擾控製器。為了驗證本文的方法，搭建了液體靜壓導軌試驗臺，並進行了相應的檢測實驗，模擬與實驗表明：在自抗擾控製環境下，試驗臺電液力伺服控製系統性能變好，油膜厚度趨於穩定。